IEEE Access
Multidisciplinary | Rapid Review | Open Access Journal

Received December 25, 2017, accepted March 16, 2018, date of publication April 4, 2018, date of current version May 2, 2018.

Digital Object Identifier 10.1109/ACCESS.2018.2820689

An Extended Model for Fatigue Life Prediction and Acceleration Considering Load Frequency Effect

YIKUN CAI[1], YU ZHAO[2], XIAOBING MA[1], ZHENYU YANG[3], AND YING DING[1]

[1]School of Reliability and Systems Engineering, Beihang University, Beijing 100191, China
[2]Key Laboratory of Reliability and Environmental Engineering Technology, Beijing 100191, China
[3]Institute of Solid Mechanics, Beihang University, Beijing 100191, China

Corresponding author: Xiaobing Ma (maxiaobing@buaa.edu.cn)

This work was supported in part by the National Natural Science Foundation of China under Grant 61473014 and Grant 11672014 and in part by the Fundamental Research Funds for the Central Universities.

ABSTRACT With consideration of the load frequency effect of constant-amplitude fatigue test, a fatigue acceleration technique is developed in this paper. Load frequency shows effects on both macroscopic mechanical properties and microscopic deformation behaviors of material. Thus it is necessary to take the load frequency effects into consideration in the fatigue life prediction models. In this paper, an extended model based on the S-N approach is proposed to consider the frequency effect. Fatigue life is predicted with a heteroscedastic method, and then the acceleration by increasing load frequency and stress amplitude is studied. The presented model is also validated by a comparison between the theoretical prediction and experimental results. It is shown that the presented model is consequential in improving the S-N curves obtained under various load frequencies. In addition, load frequency increasing can lead to effective acceleration although the retardant effect is also triggered due to the increase of deformation resistance.

INDEX TERMS Fatigue life prediction, accelerated factor, frequency effect, *P-S-N* curve, constant amplitude fatigue.

I. INTRODUCTION

The cyclic load is a common cause of the fatigue failure of power transmission components. Thus the constant-amplitude (CA) test, the variable-amplitude (VA) test, and the random vibration test are conducted to test components' fatigue life. The CA fatigue test is considered as the fastest, most straightforward, least expensive, and most frequently used fatigue test method in laboratory. However, it is still expensive and time consuming, which results from the tentative test procedures, especially for high-reliable components.

Fortunately, the accelerated test techniques can provide a solution to this problem. For the constraints of time and expense, in order to evaluate the product performance under service load in a relatively short time, acceleration is conducted under harsher load spectrum within the mechanism consistency boundary in the laboratory. The most frequently studied acceleration issues include acceleration techniques under single stress like temperature, humidity, random vibration or their combination. However, only a few studies were focused on the aspect of accelerated fatigue test modeling and life prediction.

For example, under random vibration load condition, Pothula *et al.* [1] involved aluminum beams subjected to accelerated random vibration. The experimentally observed failure time was used to examine the performance of various fatigue failure theories. Allegra and Zhang [2] addressed the use of inverse power laws in accelerated fatigue test under wide-band Gaussian random load to evaluate the fatigue damage relative accumulation. Under CA load condition, damage based models for step-stress accelerated life test were studied [3] and an acceleration concept considering stress ratio effect based on the Paris Law was proposed [4]. As for VA load condition, carrier cycles make up a big part of the load history while making little contribution to fatigue damage. A good idea for acceleration is to generate an equivalent load history by filtering out the carrier cycles [5]. Lin *et al.* [6] qualitatively compared two different approaches for predicting fatigue limit distributions based on computer

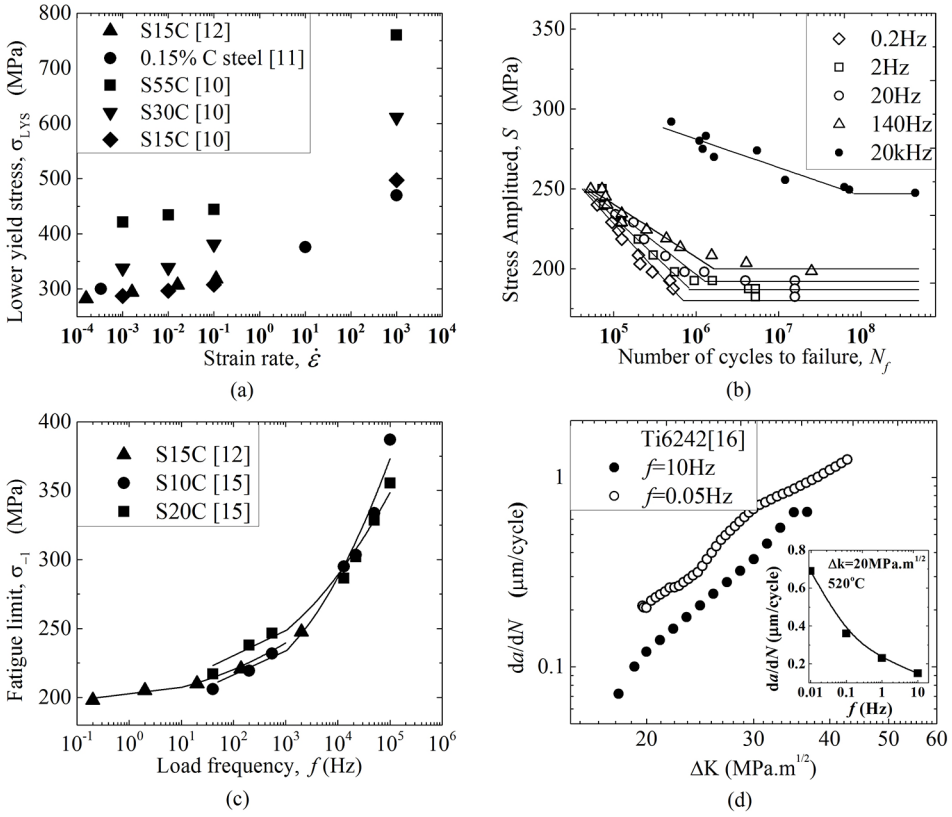

FIGURE 1. Load frequency effect. (a) The linear relationship between lower yield stress and strain rate [10]–[12]; (b) *S-N* diagram of S15C steel under several load frequencies [12]; (c) The dependence of fatigue limit on load frequency obtained in [12] and [15]; (d) Crack growth rate under different load frequencies [16].

simulations. The above-mentioned works involved the load stress as the fatigue driving force. Innovative energy parameter approach was also suggested as a new way to study fatigue issues. For instance, a modified energy activation model was built by Kim and Lu [7], in which the temperature and stress were considered as fatigue acceleration factors. In addition, an energy parameter considering normal and shear deformation was used to predict fatigue life under VA multi-axial load and a linear relationship between fatigue life and energy parameter was built in a log-log coordinate [8].

Reasons for the insufficient study of accelerated fatigue test are as follows: (a) complexity of the fatigue progress; (b) complication of the load spectrum effect; (c) lack of proper acceleration models; and (d) inadequate study of the failure mechanism consistency.

In this paper, a practical and general life prediction method is proposed for accelerated constant-amplitude fatigue test, with quantitative characterization of the load frequency effect. A detail discussion of the load frequency effect is conducted in section II, followed by a brief review of existing fatigue life prediction models and the construction of the newly proposed models in section III. Section IV validates the performance of the fatigue life prediction model considering the frequency effect. Acceleration considering frequency effect is discussed in section V. Some important conclusions are summarized in the last section.

II. FREQUENCY EFFECT ON CONSTANT-AMPLITUDE FATIGUE TEST

Load frequency has different impacts on the mechanical properties of various materials. Actually, the load frequency effect is manifested as the strain rate effect, which is more widely studied. As for high-strength steels, the effect of load frequency is not obvious [9]. However, for materials such as low carbon steel, the frequency effect is significant and worthy to be noted. Generally, load frequency effect could be stated in two aspects: the macroscopic mechanical properties and the microscopic fatigue deformation behavior.

A. FREQUENCY EFFECT ON THE MACROSCOPIC MECHANICAL PROPERTIES

Itabashi and Kawata [10] tested seven kinds of structural carbon steel at four strain rates of 1×10^{-3}, 1×10^{-2}, 1×10^{-1} and $1\times10^{3}\mathrm{s}^{-1}$ under monotonic load. The tensile strength, lower yield strength, and proportional limit were found to increase with the increase of strain rate. For a strain rate range of 10^{-3}-$10^{-1}\mathrm{s}^{-1}$, a linear relationship between stress and the logarithm of strain rate was illustrated in Fig. 1 (a). The same increase trend of frequency effect on stress was

also investigated in [11]–[13] and linear relationships were demonstrated [11], [12].

Under cyclic load, it was investigated by several works that both the fatigue strength and fatigue life increase with the increase of the load frequency [11]–[15]. Fatigue tests were carried out on JIS S15C low carbon steel in a wide range of load frequency from 0.2 Hz to 20 kHz [12]. The frequency effect on the *S–N* property was examined and shown in Fig. 1. (b). The fatigue limit σ_{-1} was also found to increase with the increase of load frequency, and similar results can be found in [15] (shown in Fig. 1. (c)). In [13], the cyclic proportional limit (the departure point from the linear stress-strain relation) increased with the increase of load frequency. Sansoz and Ghonem [16] studied the frequency effect from a viewpoint of the crack growth. They conducted several experiments on Ti6242 alloy under different fatigue load frequencies and found that the crack growth rate da/dN increased with the increase of load frequency, as shown in Fig. 1. (d).

B. FREQUENCY EFFECT ON THE MICROSCOPIC FATIGUE DEFORMATION BEHAVIOR

On the other hand, some researchers focused on the fatigue deformation behavior and tried to give an insight into the failure mechanism on a microscopic scale. It was found that the total hysteresis energy up to failure was not sensitive to the load frequency although the hysteresis energy distributed very differently in the whole test period [12]. Energy loss was considered to reflect the fatigue damage because the accumulated fatigue damage probably affects the shape and area of the hysteresis loop throughout the fatigue test [17]. Sugimoto and Sasaki [14] found that energy loss per cycle under the load frequency of 5 Hz was smaller than that under 0.5 Hz. Lee and Liu [18] conducted experiments on three kinds of steel under strain rates ranging from 1.1×10^3 s^{-1} to 5.5×10^3 s^{-1}. The results indicated that the cyclic hardening exponent decreased with the increase of strain rate whereas the dislocation density increased. The measurement technique of very high-frequency response was employed in the study [10] in order to learn how much work has converted into heat. Absorbed energy per unit volume, a measure of toughness, increased in the strain rate range of 10^{-3}-$10^3 s^{-1}$ and it agrees with the theoretically calculated value of the increasing trend of temperature rise [18].

Based on experimental investigations, the load frequency effect (strain rate effect) can be explained by the plastic deformation mechanism. Higher strain rate produces the higher density of dislocations inside cell walls with smaller size [18]. This fact leads to a smaller mobility of dislocations at the higher strain rate. Thus it will be more difficult for plastic deformation phenomenon to happen. When the load frequency increases, the slip line density increases and the size of the reversed plastic zone at the crack tip decreases [16], resulting in increased cross-slip interactions and lower crack growth rates.

In recent years, attention has been given to the fatigue behavior of metals in the region up to 10^7 cycles, which is called Very High Cycle Fatigue (VHCF) [9], [19]. The ultrasonic fatigue test method has often been applied to investigate the fatigue properties [12]. It is conducted at a very high load frequency (around 2 kHz) and is able to obtain the fatigue properties in a much shorter time than commonly used test method (in the range of 1-100 Hz). It is an effective way to accelerate the fatigue test but there exists a huge gap between the ultrasonic fatigue test method and the conventional fatigue test method. For example, the fatigue behavior of some materials like high-strength steels, case-hardened steels, and aged titanium alloys are very different [19]. It has been proved that there is no fatigue limit and the *S-N* curve decreases continuously in the very long life region up to 10^7 to 10^8 cycles. The fatigue failure occurs at small internal defects in subsurface zones instead of the specimen surface. Moreover, the fatigue behavior may also be changed because material condition changes due to heat generation during ultrasonic fatigue test. Thus, in this paper we discuss the frequency effect of materials for common purposes within conventional fatigue life ($<10^7$ cycles) and load frequency (<1000 Hz).

III. FATIGUE LIFE PREDICTION MODELS

A. GENERAL MODELS

During the past decades, quite a number of models have been proposed for fatigue life prediction. Generally, these models can be classified into three categories: fatigue life based models, damage based models and crack growth based models.

The most widely used method of fatigue behavior modeling is the graphical illustration with the aid of a stress-life (*S-N*) or strain-life (ε-*N*) curve. In most cases, a linear fitting of stress and fatigue life can be obtained in a log-log or semi-log coordinate. It usually only represents the total fatigue life and is impossible to distinguish between crack initiation and propagation phase. Actually, *S-N* curve can be considered as a kind of acceleration method because engineers can conduct fatigue tests under a higher stress level and predict actual fatigue life under service stress with the linear relation.

Damage based models are proposed as an extension to be used under varied amplitude fatigue load condition. The basic idea of damage based models is that fatigue damage (crack size or crack density) accumulates in each cycle, and failure occurs when the sum of damage D reaches 1.0. The first and simplest model is known as the Miner's damage rule [20], which assumes a linear relation between the accumulated damage D and the load cycles n_c with a slope of $1/N_f$. This linear damage model can be expressed as

$$D = \frac{n_c}{N_f} \tag{1}$$

where N_f is the fatigue life in cycles. Miner's rule is based on the assumption of load sequence independence. It was proved

to be inaccurate under complicated load sequences. Thus the bilinear model [21] was proposed to consider the distinction of damage accumulation in crack initiation and propagation phases, and the damage curve analysis relation [21] was proposed to take into account the effect of load history on damage accumulation. Some other methodologies were also developed such as the probabilistic damage model with the consideration of both material and load dispersion.

Crack growth based models are commonly inspired by the observation of crack growth rate under various crack driving force such as the stress intensity factor range ΔK. A simple and well-known method for predicting fatigue crack propagation is the Paris Law. A comprehensive overview of models considering the stress ratio effect and load sequence interaction effect can be found in [22] and [23].

B. HUNG'S MULTI-PARAMETER MODEL

None of the above-mentioned models has focused on the modeling of load frequency effect. In fact, an *S-N* curve can be extrapolated to include the influence of geometry, chemical environment, load frequency, temperature and mean stress with the knowledge of how they affect the *S-N* curve. For example, Hung and Hong [24] proposed a multi-parameter model considering the effects of both the applied stress and the load frequency, which can be expressed as

$$N_f = \alpha \times S^{\beta} \times f^{\eta} \tag{2}$$

where N_f is the number of cycles to failure, S is the applied stress, f is the load frequency, and, α, β and η are constants. The logarithm of Eq. (2) is

$$\lg N_f = \lg \alpha + \beta \lg S + \eta \lg f \tag{3}$$

It implies that the *S-N* curves are parallel under the log-log coordinate with a shift factor proportional to $\lg f$. This was also suggested in Guennec *et al.*'s study [12], in which the *S-N* curves of different load frequencies were condensed to a small range around a universal curve.

C. AN EXTENDED MODEL CONSIDERING THE LOAD FREQUENCY EFFECT

A further look into the curves obtained under different load frequencies for various materials [12], [14], [15] showed that the slope β is not constant. The Hung's model and the condensed universal curve did not fit experimental data very well because of the interaction between the applied stress and the load frequency. Thus, a new model is needed to consider the load frequency effect on both the intercept and the slope of the *S-N* curve.

Herein, based on the theoretical knowledge and experimental observations, a new model considering the load frequency effect can be constructed. As discussed in section II. A, the fatigue mechanical properties were found monotonically related to the load frequency. A good linear relation between the fatigue limit σ_{-1} and the logarithm of the load frequency $\lg f$ was demonstrated in [11]–[13] and [15]. The correlation coefficient R is calculated to evaluate the accuracy of the linear relation with experimental data from [11]–[13] and [15]. The values of R are higher than 0.95 for all the four references and indicates high goodness-of-fit for the linear relation. The slope of the *S-N* curve is also linearly related to the load frequency [12], [14], [15] with R higher than 0.93.

Thus, based on the *S-N* approach, an extended model considering the frequency effect can be proposed under the following assumptions:

1) Linear relationship between fatigue limit σ_{-1} and $\lg f$;

2) Linear relationship between slope k_0 and $\lg f$;

3) All fatigue tests are conducted within the stress range of lower bound σ_L and upper bound σ_U, where $\sigma_L = \sigma_{-1}$ is the fatigue limit and σ_U is the maximum stress allowed for the fatigue test.

4) Fatigue life data under very high load frequency or longer than 10^7 cycles are not included in the model, because the fatigue behavior is different from the conventional fatigue test results.

Then the model can be expressed as

$$\lg S = \sigma_{-1} + k_0 \lg N_f \tag{4}$$

$$\sigma_{-1} = a_1 + b_1 \lg f \tag{5}$$

$$k_0 = a_2 + b_2 \lg f \tag{6}$$

where k_0, a_1, b_1, a_2 and b_2 are constants determined by experimental data. Substitute Eqs. (5) and (6) into Eq. (4), the model comes to the following

$$\lg S = \alpha_1 + \beta_1 \lg f + \beta_2 \lg N_f + \beta_3 \lg f \lg N_f \tag{7}$$

It can also be rewritten as

$$\lg S = \alpha_1 + \beta_1 \lg f + (\beta_2 + \beta_3 \lg f) \lg N_f \tag{8}$$

where α_1, β_1, β_2 and β_3 are constants determined by experimental data. It accounts for the interaction between the applied stress and the load frequency with a multiplicative term $\beta_3 \lg f \lg N_f$.

IV. FATIGUE LIFE PREDICTION

A. VALIDATION OF THE EXTENDED MODEL

Two models considering the load frequency effect, Hung's model and the extended model have been given in Eqs. (2)-(8). The *S-N* properties under different frequencies (within usual frequency range) of three materials from previous studies are examined graphically as shown in Figs. 2-4. The experimental materials are listed in TABLE 1.

For JIS S15C low carbon steel, fatigue tests were carried out under the load frequency of 0.2 Hz, 2 Hz, 20 Hz and 140 Hz in [12]. The *S-N* properties of the two models are examined and shown in Fig. 2. Fatigue life higher than 10^6 cycles is demonstrated free of fatigue failure and is not included in the model. As shown in TABLE 1, the slopes of the *S-N* curves increase with load frequency, while the curves

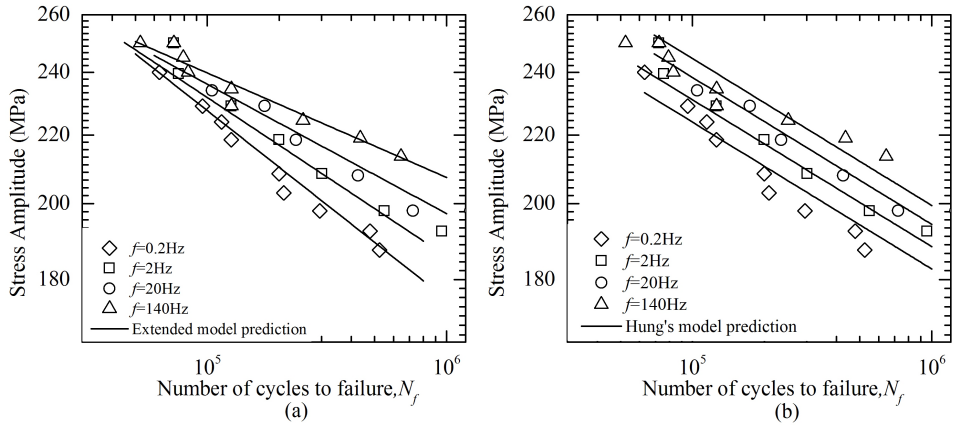

FIGURE 2. *S-N* curves for JIS S15C low carbon steel [12] obtained by (a) the extended model; (b) Hung's model.

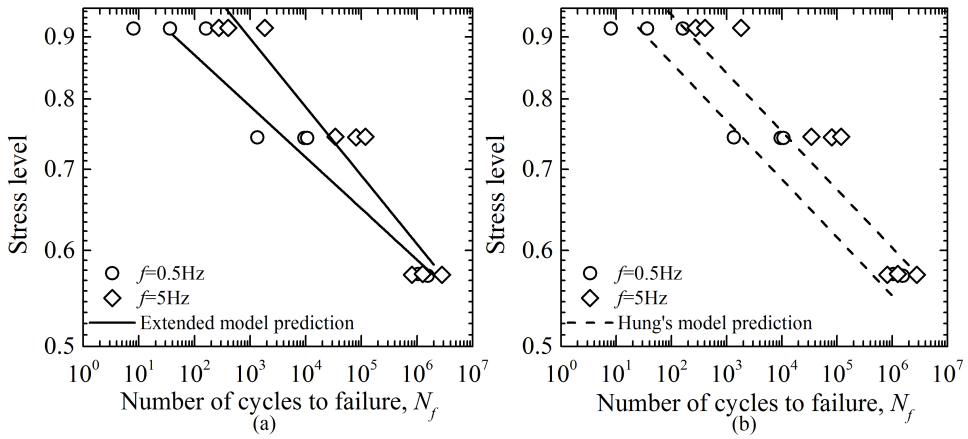

FIGURE 3. *S-N* curves for JAS structural plywood [14] obtained by (a) the extended model; (b) Hung's model.

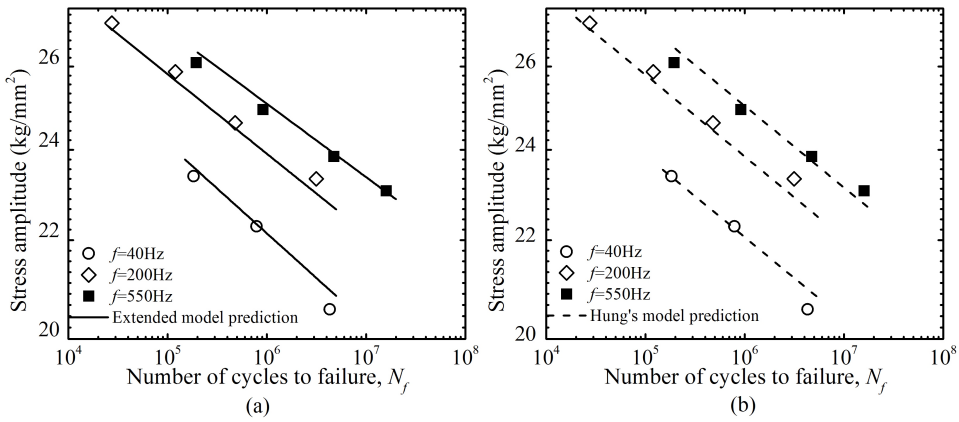

FIGURE 4. *S-N* curves for S10C low carbon steel [15] obtained by (a) the extended model; (b) Hung's model.

did not fit data well under 0.2 Hz (◊) and 140 Hz (Δ) as shown in Fig. 2 (b).

For JAS structural plywood [14], two load frequencies (0.5 Hz, 5 Hz) are examined. The slopes of the *S-N* curves decrease with load frequency increasing (in TABLE 1). The extended model is able to account for the slope variation and the Hung's model obtains parallel curves (Fig. 3).

For S10C low carbon steel in [15], specimens are tested under 40 Hz, 200 Hz, and 550 Hz. As shown in TABLE 1, the slopes of the *S-N* curves increase monotonically with

TABLE 1. Materials for model validation.

Material	Ref.	*S-N* curves	Load frequency (Hz)	Slope
JIS S15C low carbon steel	[12]	Fig. 2	0.2	-0.114
			2	-0.096
			20	-0.078
			140	-0.063
JAS structural plywood	[14]	Fig. 3	0.5	-0.042
			5	-0.056
S10C low carbon steel	[15]	Fig. 4	40	-0.043
			200	-0.034
			550	-0.031

increasing load frequency. The curves obtained by the extended model and Hung's model are given in Fig. 4, but it cannot be determined by graphical examination that which model gives the better result.

Thus the Akaike information criterion (AIC), the correct Akaike information criterion (AIC_C) and the Bayesian information criterion (BIC) are introduced to examine the performance of the two models. All of these criteria are balance between goodness-of-fit and model complexity with

$$AIC = 2k + n \cdot \ln(\frac{RSS}{n}) \tag{9}$$

$$AIC_C = \frac{2n}{n-k-1} \cdot k + n \cdot \ln(\frac{RSS}{n}) \tag{10}$$

$$BIC = \ln(n) \cdot k + n \cdot \ln(\frac{RSS}{n}) \tag{11}$$

where k is the number of parameters in the model, n is the sample size, and RSS is the residual sum of square

$$RSS = \sum_{i=1}^{n} (\lg S_i - \lg S_i')^2 \tag{12}$$

where S_i and S_i' are the i^{th} point of the *S-N* curves obtained by experiment and model prediction, respectively.

AIC, AIC_C, and BIC consider the complexity of the model as a selection criterion and essentially penalize the likelihood, based on the number of parameters in the model and the sample size. The penalty coefficient for AIC is constant 2, while that of AIC_C is $2n/(n-k-1)$, which decreases with sample size. On the contrary, the penalty coefficient of BIC is $\ln(n)$, which increases with sample size. When applying these criteria to the previously proposed models, the best one is the model with the lowest value of the AIC, AIC_C, or BIC.

It is seen (in TABLE 2) that the model proposed in this paper is more successful in correlating the *S-N* curves obtained under various load frequencies when the slopes of the *S-N* curves increase/decrease monotonically with increasing load frequency. For example, for the JIS S15C low carbon steel [12], the predicted curves fit the experimental data well with slopes of -0.114, -0.096, -0.078 and -0.063 under 0.2 Hz, 2 Hz, 20 Hz, and 140 Hz, respectively. The extended model shows better performance with both a higher R-square and lower AIC, AIC_C, and BIC. That means the load frequency effect on fatigue life is significant and should be considered.

TABLE 2. AIC, AIC_C, and BIC for different models.

Ref.	Model	R-square	*AIC*	*BIC*	AIC_C
[12]	Hung's	0.9339	-280.5	-276.2	-279.6
	Extended	0.9648	-296.9	-291.2	-295.4
[14]	Hung's	0.9169	-121.6	-119.1	-119.7
	Extended	0.9363	-124.1	-123.6	-120.8
[15]	Hung's	0.9808	-143.8	-142.0	-140.9
	Extended	0.9834	-143.9	-141.4	-138.2

As for the last material from [15], although the extended model is a little more accurate with a higher R-square, the AIC_C and BIC are also higher. That is because slopes variation is not significant with the change of the load frequency and the penalty of AIC_C and BIC is very severe with $\frac{2n}{n-k-1} = 3.67$ and $\ln(n) = 2.40$ ($n = 11$, $k = 4$). For this kind of situation, the performance of each model should be examined carefully with the experimental results. Which model is better depends on the user's preference to model accuracy and complexity.

B. FATIGUE LIFE PREDICTION WITH THE HETEROSCEDASTIC METHOD

Fatigue life under the same stress is always influenced by various sources of random factors and the scatter can be modeled by distributions. Engineering practice and numerous fatigue test data have demonstrated that the variance of fatigue life will linearly increase with the decrease of stress in a log-log or semi-log coordinate. The conventional homoscedastic model can overestimate the variance in the high-stress range and underestimate it in the low-stress range. Thus the heteroscedastic model is employed to measure the quantitative law of the variance change. For the *S-N* relation, let $y = \lg N_f$, $x = \lg S$, it can be expressed as

$$y = a + bx + e \tag{13}$$

$$e \sim N(0, \sigma^2(x)) \tag{14}$$

$$\sigma(x) = \sigma[1 + \theta(x - x_0)] \tag{15}$$

$$x_0 = \frac{1}{n}\sum_{i=1}^{n} x_i \tag{16}$$

where a, b, σ and θ are parameters to be estimated by the maximum likelihood estimation (MLE) method. Then the *S-N* curve can be expressed as

$$\lg \hat{N}_f = \hat{a} + \hat{b} \lg S \tag{17}$$

Because of the scatter of the fatigue data, the *P-S-N* curve is needed to make sure structures can survive from fatigue stress with high probability of p, and it can be obtained with

$$\lg N_{fp} = a_0 + b_0 \lg S - u_\gamma c_0 \hat{\sigma} \sqrt{c_1 \lg^2 S + c_2 \lg S + c_3} \tag{18}$$

where a_0, b_0, c_0, c_1, c_2 and c_3 are parameters determined by experimental data with the MLE method. $\gamma = \Phi(u_\gamma)$ is the confidence level and $\Phi(\cdot)$ is the cumulative distribution function (CDF) of the standard normal distribution.

TABLE 3. Converted fatigue life data for the JIS S15C low carbon steel [12].

Load Frequency		1	2	3	4	5	6	7	8	9
0.2Hz	lg$N$	4.80	4.98	5.06	5.10	5.30	5.32	5.47	5.68	5.72
	lg$S$	2.384	2.366	2.358	2.349	2.331	2.322	2.312	2.302	2.292
2Hz	lg$N$	4.86	4.88	5.10	5.30	5.48	5.74	5.98		
	lg$S$	2.398	2.379	2.36	2.340	2.320	2.297	2.284		
20Hz	lg$N$	5.02	5.24	5.37	5.63	5.86				
	lg$S$	2.362	2.351	2.326	2.301	2.274				
140Hz	lg$N$	4.72	4.86	4.90	4.92	5.10	5.10	5.40	5.64	5.81
	lg$S$	2.396	2.396	2.383	2.370	2.355	2.340	2.328	2.311	2.295

The*S-N* curves under different load frequencies have varied slopes. To estimate fatigue life under service load frequency, the experimental data must first be converted to a universal curve by a rotation transformation through Eq. (8). For the JIS S15C low carbon steel tested in [12], the service load frequency is assumed to be 2 Hz and the converted data are listed in TABLE 3. Then the parameters can be estimated with the heteroscedastic model.

With the heteroscedastic method, parameters are obtained with $\hat{a} = 28.184$, $\hat{b} = -9.787$, $\hat{\sigma} = 0.1055$, and $\hat{\theta} = -3.925$. The *S-N* curve is shown in Fig. 5 with linear correlation coefficient $R = -0.963$, giving by the following

$$\lg \hat{N}_f = 28.184 - 9.787 \lg S \tag{19}$$

and the *P-S-N* curve with survival rate $p = 0.99$ and confidence coefficient $\gamma = 0.95$ is also shown in Fig. 5 and can be given by

$$\lg N_{fp} = 25.534 - 8.765 \lg S - 0.184\sqrt{24.68 \lg^2 S - 116.70 \lg S + 137.96} \tag{20}$$

It is easy to understand that $\hat{\theta} = -3.925 < 0$ indicates the variation of fatigue life increases with the decrease of the applied stress. As can be seen in Fig. 5, the experimental data gathers around the *S-N* curve and are all at the right of the *P-S-N* curve and suggests that the heteroscedastic model has a good performance in fatigue data analysis.

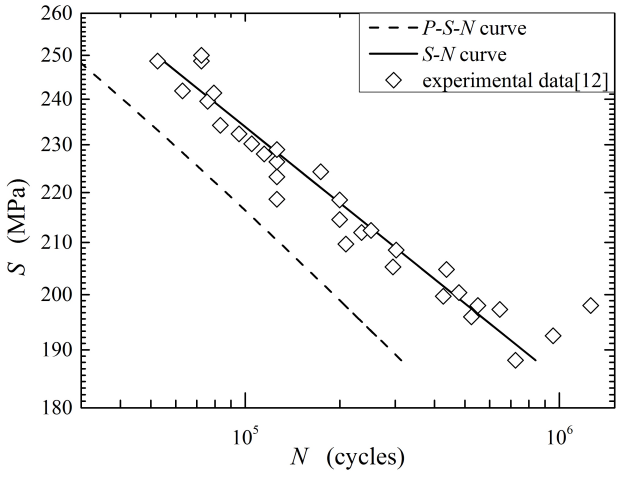

FIGURE 5. ***S-N* and *P-S-N* curve under service load frequency for JIS S15C low carbon steel [12].**

After transforming the raw data to 0.2 Hz, 20 Hz and 140 Hz, the parameters under these load frequencies are also calculated with the heteroscedastic method. The intercept a and the slope b of the *P-S-N* curve are changed under different load frequency. In a log-log coordinate, σ is the variance of fatigue life under average stress level and it remains unchanged. θ remains negative and decreases when load frequency increases because the *S-N* data are transformed to a smaller range of stress level. And θ increases when load frequency decreases because the *S-N* data are transformed to a wider range of stress level.

V. ACCELERATION ANALYSIS OF FATIGUE LIFE TEST

Fatigue failure is a process of crack initiation and propagation. Bonds breaking results in new fracture surfaces. Crack grows every cycle and failure occurs when crack length reaches a critical level, and then it turns into a rapid fracturing process. The Griffith criterion predicts that the crack tip begins to propagate when the crack tip energy release rate reaches the fracture surface energy. It indicates that the growth of crack is a competition between the crack driving force and the deformation resistance, which also suggests that the fatigue failure process can possibly be accelerated at least by the following ways:

1) Acceleration of the crack growth per unit time by increasing the load frequency; 2) Acceleration of the crack growth per cycle by increasing the crack driving force; 3) Acceleration of the crack growth per cycle by decreasing the deformation resistance.

It could not be a more straightforward idea for fatigue test acceleration by increasing the load frequency. In this work, 1) and 2) will be demonstrated in the following section while 3) is out of the scope of this work.

A. ACCELERATED FACTOR CONSIDERING THE LOAD FREQUENCY EFFECT

The accelerated factor (AF) for fatigue test is defined as the test time ratio between accelerated stress condition and

service stress condition as the following

$$AF = t_{f1}/t_{f0} \tag{21}$$

$$t_{f1} = N_{f1}/f_1, t_{f0} = N_{f0}/f_0 \tag{22}$$

where t_{f0} and t_{f1} are the failure time under service load frequency f_0 and accelerated load frequency f_1, respectively. N_{f0} and N_{f1} are cycles to failure under f_0 and f_1, respectively. Thus

$$AF = \frac{f_0}{f_1} \cdot \frac{N_{f1}}{N_{f0}} = R_f \cdot AF_0 \tag{23}$$

where $R_f = f_0/f_1$ is the load frequency ratio and $AF_0 = N_{f1}/N_{f0}$ is the relative accelerated factor accounting for the load frequency effect.

As the heteroscedastic method implied, the logarithm of the fatigue life is normally distributed following

$$\lg N_f \sim N(a + bx, \sigma^2[1 + \theta(x - x_0)]^2) \tag{24}$$

where $x = \lg S$. Let $\mu = a + bx$, $\sigma(x) = \sigma[1 + \theta(x - x_0)]$, thus

$$\lg N_f \sim N(\mu, \sigma^2(x)) \tag{25}$$

From Eq. (23) we can obtain

$$\lg AF_0 = \lg \frac{N_{f1}}{N_{f0}} = \lg N_{f1} - \lg N_{f0} \tag{26}$$

Thus

$$\lg AF_0 \sim N(\mu_1 - \mu_0, \sigma_1^2 + \sigma_0^2) \tag{27}$$

where μ_1 and μ_0 are the average logarithmic fatigue life under load frequency f_1 and f_0. σ_1^2 and σ_0^2 are the variance. Considering the scatter of experimental data, the lower confidence limit of $\lg AF_0$ can be given by

$$\lg AF_{0L} = \mu_1 - \mu_0 - \sqrt{\sigma_1^2 + \sigma_0^2} \cdot u_\gamma \tag{28}$$

The lower confidence limit of AF is

$$AF_L = R_f \cdot 10^{\mu_1 - \mu_0 - \sqrt{\sigma_1^2 + \sigma_0^2} \cdot u_\gamma} \tag{29}$$

The effect of two acceleration programs are examined graphically in Fig. 6 and Fig. 7 for JIS S15C low carbon steel [12]. The relative accelerated factor AF_0 is the ratio of cycles to failure and the real accelerated factor AF is the ratio of times to failure between the accelerated and service load conditions.

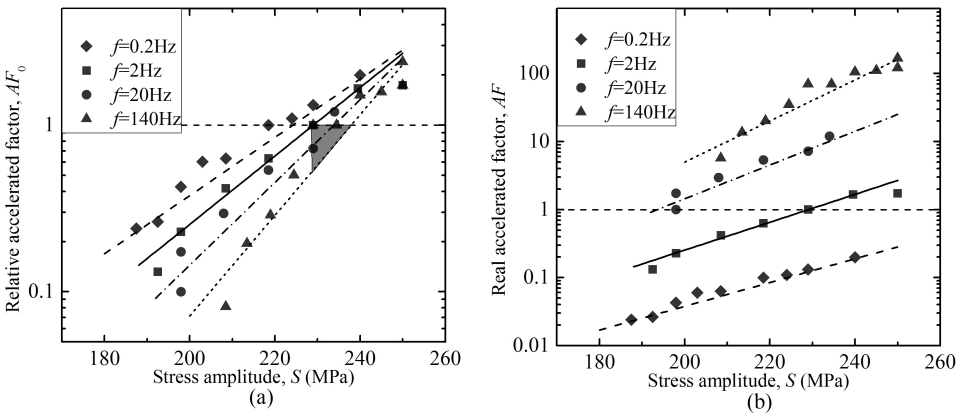

FIGURE 6. AF_0 and AF when change load frequency for JIS S15C low carbon steel [12].

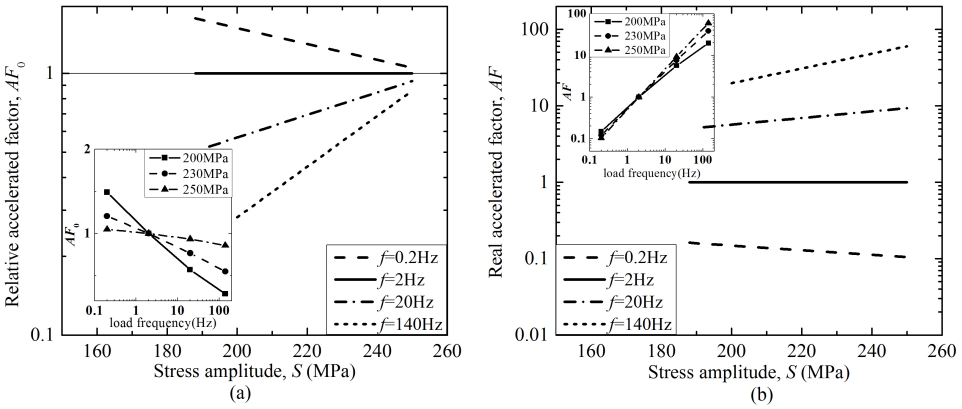

FIGURE 7. AF_0 and AF when change both load frequency and stress amplitude for JIS S15C low carbon steel [12].

TABLE 4. AF_0 and AF when change load frequency under 200MPa and 250MPa for JIS S15C low carbon steel [12].

Load frequency	200MPa		250MPa		f_i/f_2
	AF_0	AF	AF_0	AF	
0.2Hz	1.49	0.15	1.05	0.105	0.1
2Hz	1	1	1	1	1
20Hz	0.57	5.69	0.93	9.34	10
140Hz	0.28	19.7	0.86	60.08	70

Fig. 6 illustrates the acceleration effect by changing load frequency under various levels of service load stress ranged between the fatigue limit and 250 MPa.

Assuming that the service load frequency is 2 Hz, the relative accelerated factor AF_0 is greater than 1.0 under 0.2 Hz and smaller than 1.0 under 20 Hz and 140 Hz (Fig. 6. (a) and TABLE 4). It is seen that under the same stress amplitude, the increase of load frequency results in the decrease of the relative accelerated factor AF_0. It is caused by the increase of deformation resistance induced by higher dislocation density under higher strain rate. When the service stress is 200 MPa, AF_0 is 1.49, 0.57 and 0.28 for 0.2 Hz, 20 Hz and 140 Hz respectively, suggesting that the load frequency effect is significant in the low-stress region. When the service stress increases, AF_0 under four load frequencies approaches to 1.0 and the difference of AF_0 is smaller in the high-stress region. When the service stress is 250 MPa, AF_0 is 1.05, 0.93 and 0.86 for 0.2 Hz, 20 Hz and 140 Hz, respectively. This is because the dislocation introduced by higher stress amplitude plays the main role in the deformation resistance and the load frequency effect is relatively weakened.

The real accelerated factor AF is a vertical shift of AF_0 with the factor $\lg f$ on the log-log plot. AF is smaller than 1.0 under 0.2 Hz and greater than 1.0 under 20 Hz and 140 Hz (Fig. 6. (b)). When stress is 250 MPa, AF is 0.105, 9.34 and 60.08 when AF_0 is 1.05, 0.93 and 0.86 for 0.2 Hz, 20 Hz and 140 Hz, respectively. It implies that it is still positive in saving test time to increase the load frequency although the deformation resistance is also increased.

Fig. 7 shows the acceleration effect by increasing both the load frequency and the stress amplitude. The service stress amplitude is assumed to be 230 MPa and the load frequency to be 2 Hz. AF_0 increases from the low-stress region to the high-stress region due to the increasement of crack driving force (Fig. 7 (a)). In the shadowed region, the acceleration effect of stress increasing is faded by the retardation effect of increasing the load frequency. In Fig. 7. (b), AF is greater than 1.0 under 20 Hz and 140 Hz even in the low-stress region and smaller than 1.0 under 0.2 Hz even in the high-stress region. It indicates that increasing load frequency is promising for fatigue acceleration even though the retardation effect is also triggered. As can be found in TABLE 5, both increasing the stress amplitude and increasing the load frequency are feasible acceleration method and their combination is even better.

The lower confidence limit of the accelerated factor is also calculated, as shown in Fig. 8. It is seen that the AF obtained from the experimental data are all within the predicted AF lower bound, which implies good prediction performance of the method.

TABLE 5. Real accelerated factor (AF) when change both load frequency and stress amplitude for JIS S15C low carbon steel [12].

Load frequency	200MPa	230MPa	250MPa
0.2Hz	0.04	0.13	0.28
2Hz	0.25	1	2.70
20Hz	1.44	8.03	25.2
140Hz	5.01	40.3	162

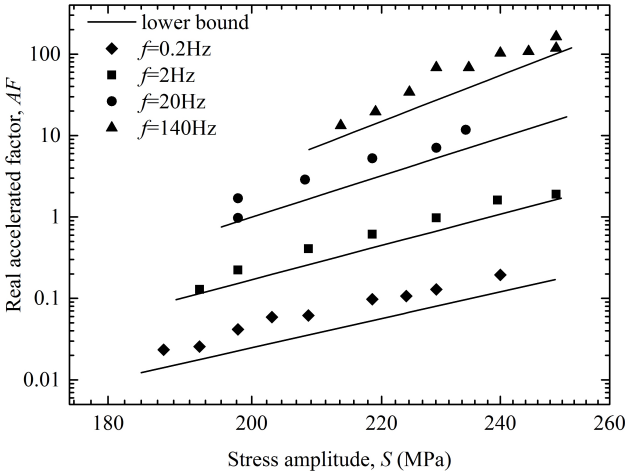

FIGURE 8. The lower confidence limit of the accelerated factor for JIS S15C low carbon steel [12].

B. FAILURE MECHANISM CONSISTENCY

The guarantee of failure mechanism consistency is the fundamental of the accelerated test. It should be noted that the proposed model may be used only to consolidate the *S-N* properties in the usual frequency region (0.2-550 Hz in this paper). The frequency effect in very high and low frequency regions is rather complicated and remains to be further explored because anomalous phenomenon may occur beyond the usual frequency region [24], [25]. In high frequency fatigue test, temperature rises in the high strain rate adiabatic deformation process because a significant proportion of the plastic work is converted into heat [18]. The rise in temperature may result in the change of material condition. In [12], ultrasonic tests (around 20 kHz) were conducted and the *S-N* property was significantly different from the properties of the low frequency range (Fig. 1. (b)). As for the low-cycle fatigue test, it is known that the deformation zone becomes bigger and distributes more evenly when frequency decreases [26]. Unfortunately, it is not very clear where exactly the boundaries of these three regions are. On the other hand, the stress amplitude range can be set as (σ_{-1}, σ_{LYS}) which can be determined with Eq. (5).

It should also be noted that, like most models for fatigue issues, the proposed model is based on the observation of

the fatigue behavior and should be examined carefully for different materials and various data types.

VI. CONCLUSIONS

Based on a recapitulative summary of the load frequency effect on material fatigue properties in constant-amplitude fatigue test, an extended model considering the load frequency effect is developed for fatigue life prediction and the predicted results are consistent with experiments.

The model is used to demonstrate the acceleration effect of load frequency and stress amplitude. It is suggested that, although the acceleration factor is reduced by the increased crack propagation resistance caused by the load frequency effect, it cannot be completely eliminated. It is feasible and effective to conduct accelerated fatigue test by increasing load frequency and stress amplitude.

REFERENCES

[1] A. Pothula, A. Gupta, and G. R. Kathawate, "Fatigue failure in random vibration and accelerated testing," *J. Vibrat. Control*, vol. 18, no. 8, pp. 1199–1206, Jul. 2012.

[2] G. Allegri and X. Zhang, "On the inverse power laws for accelerated random fatigue testing," *Int. J. Fatigue*, vol. 30, no. 6, pp. 967–977, Jun. 2008.

[3] Y. Lee and M. Lu, "Damage-based models for step-stress accelerated life testing," *J. Test. Eval.*, vol. 34, no. 6, pp. 494–503, 2006.

[4] F. Guerin, B. Dumon, R. Hambli, and O. Tebbi, "Accelerated testing based on a mechanical-damage model," in *Proc. RAMS*, Jan. 2001, pp. 372–376.

[5] J. J. Xiong and R. A. Shenoi, "A load history generation approach for full-scale accelerated fatigue tests," *Eng. Fract. Mech.*, vol. 75, no. 10, pp. 3226–3243, Jul. 2008.

[6] S.-K. Lin, Y.-L. Lee, and M.-W. Lu, "Evaluation of the staircase and the accelerated test methods for fatigue limit distributions," *Int. J. Fatigue*, vol. 23, no. 1, pp. 75–83, Jan. 2001.

[7] G.-H. Kim and H. Lu, "Accelerated fatigue life testing of polycarbonate at low frequency under isothermal condition," *Polym. Test.*, vol. 27, no. 1, pp. 114–121, Feb. 2008.

[8] B. L. Lee, K. S. Kim, and K. M. Nam, "Fatigue analysis under variable amplitude loading using an energy parameter," *Int. J. Fatigue*, vol. 25, no. 7, pp. 621–631, Jul. 2003.

[9] T. Sakai, "Review and prospects for current studies on very high cycle fatigue of metallic materials for machine structural use," *J. Solid Mech. Mater. Eng.*, vol. 3, no. 3, pp. 425–439, 2009.

[10] M. Itabashi and K. Kawata, "Carbon content effect on high-strain-rate tensile properties for carbon steels," *Int. J. Impact Eng.*, vol. 24, no. 2, pp. 117–131, Feb. 2000.

[11] N. Tsuchida, H. Masuda, Y. Harada, K. Fukaura, Y. Tomota, and K. Nagai, "Effect of ferrite grain size on tensile deformation behavior of a ferrite-cementite low carbon steel," *Mater. Sci. Eng. A*, vol. 488, nos. 1–2, pp. 446–452, Aug. 2008.

[12] B. Guennec, A. Ueno, T. Sakai, M. Takanashi, and Y. Itabashi, "Effect of the loading frequency on fatigue properties of JIS S15C low carbon steel and some discussions based on micro-plasticity behavior," *Int. J. Fatigue*, vol. 66, pp. 29–38, Sep. 2014.

[13] I. Nonaka, S. Setowaki, and Y. Ichikawa, "Effect of load frequency on high cycle fatigue strength of bullet train axle steel," *Int. J. Fatigue*, vol. 60, pp. 43–47, Mar. 2014.

[14] T. Sugimoto and Y. Sasaki, "Effect of loading frequency on fatigue life and dissipated energy of structural plywood under panel shear load," *Wood Sci. Technol.*, vol. 40, no. 6, pp. 501–515, Aug. 2006.

[15] M. Kikukawa, K. Ohji, and K. Ogura, "Push-pull fatigue strength of mild steel at very high frequencies of stress up to 100 kc/s," *J. Soc. Mech. Eng. Int. J. Ser. A*, vol. 32, no. 235, pp. 363–370, 1966.

[16] F. Sansoz and H. Ghonem, "Effects of loading frequency on fatigue crack growth mechanisms in α/β Ti microstructure with large colony size," *Mater. Sci. Eng. A*, vol. 356, nos. 1–2, pp. 81–92, Sep. 2003.

[17] C. L. Hacker and M. P. Ansell, "Fatigue damage and hysteresis in wood-epoxy laminates," *J. Mater. Sci.*, vol. 36, no. 3, pp. 609–621, Feb. 2001.

[18] W.-S. Lee and C.-Y. Liu, "The effects of temperature and strain rate on the dynamic flow behaviour of different steels," *Mater. Sci. Eng. A*, vol. 426, nos. 1–2, pp. 101–113, Jun. 2006.

[19] K. Shiozawa and L. T. Lu, "Internal fatigue failure mechanism of high strength steels in gigacycle regime," *Key Eng. Mater.*, vols. 378–379, pp. 65–80, Mar. 2008.

[20] M. A. Miner, "Cumulative damage in fatigue," *J. Appl. Mech.*, vol. 67, pp. A159–A164 Feb. 1945.

[21] S. S. Manson and G. R. Halford, "Practical implementation of the double linear damage rule and damage curve approach for treating cumulative fatigue damage," *Int. J. Fract.*, vol. 17, no. 2, pp. 169–192, Apr. 1981.

[22] T. Machniewicz, "Fatigue crack growth prediction models for metallic materials," *Fatigue Fract. Eng. Mater. Struct.*, vol. 36, no. 4, pp. 293–307, 2013.

[23] S. M. Beden, S. Abdullah, and A. K. Ariffin, "Review of fatigue crack propagation models for metallic components," *Eur. J. Sci. Res.*, vol. 28, no. 3, pp. 364–397, 2009.

[24] J.-N. Hung and H. Hocheng, "Frequency effects and life prediction of polysilicon microcantilever beams in bending fatigue," *J. Micro/Nanolithogr. MEMS MOEMS*, vol. 11, no. 2, p. 021206, May 2012.

[25] X. Zhu, J. W. Jones, and J. E. Allison, "Effect of frequency, environment, and temperature on fatigue behavior of E319 cast aluminum alloy: Stress-controlled fatigue life response," *Metall. Mater. Trans. A*, vol. 39A, no. 11, pp. 2681–2688, Nov. 2008.

[26] N. Tsutsumi, Y. Murakami, and V. Doquet, "Effect of test frequency on fatigue strength of low carbon steel," *Fatigue Fract. Eng. Mater. Struct.*, vol. 32, no. 6, pp. 473–483, 2009.

YIKUN CAI received the B.S. degree from Beihang University in 2013, where he is currently pursuing the Ph.D. degree with the School of Reliability and Systems Engineering. His research interests include fatigue life assessment, atmospheric corrosion prediction, and reliability data analysis.

YU ZHAO received the Ph.D. degree from Beihang University in 2005. He is currently a Professor with the School of Reliability and Systems Engineering, Beihang University. He is also the Associate Director of the Key Laboratory on Reliability and Environmental Engineering Technology with Beihang University. His research interests include reliability engineering, reliability evaluation and verification techniques, quality management, and application of statistics techniques.

XIAOBING MA received the Ph.D. degree from Beihang University in 2006. He is currently a Professor with the School of Reliability and Systems Engineering, Beihang University. He is also a Research Fellow with the Key Laboratory on Reliability and Environmental Engineering Technology, Beihang University. His research interests include reliability data analysis, durability design, and system life modeling.

ZHENYU YANG received the B.S. and M.S. degrees from Beihang University in 2001 and 2004, respectively, and the Ph.D. degree from the Chinese Academy of Sciences in 2008. He is currently an Associate Professor with the School of Aeronautic Science and Engineering, Beihang University. His recent research interests include mechanics and physics of nano-structured materials and carbon fiber reinforced composites, and their applications in aeronautics and astronautics engineering.

YING DING received the B.S. degree from the University of Science and Technology Beijing in 2016. He is currently pursuing the master's degree with the School of Reliability and Systems Engineering, Beihang University. His research interests include life assessment of aged rubber and reliability modeling and analysis.